# Ground Water to Surface Water: Chemistry of Thermal Outflows in Yellowstone National Park

D. Kirk Nordstrom* | James W. Ball | R. Blaine McCleskey

U.S. Geological Survey

*Corresponding Author:
U.S. Geological Survey
3215 Marine St., Suite E-127
Boulder, CO 80303

Phone: 303.541.3037 Fax: 303.447.2505 Email: dkn@usgs.gov

## ABSTRACT

Geothermal waters in the earth's subsurface boil with steam separation and may mix with dilute ground waters (that may or may not contain sulfuric acid from sulfur oxidation), resulting in a wide range of compositions when they discharge and emerge at the surface. As they discharge onto the ground surface they undergo evaporative cooling, degassing, oxidation, and mineral precipitation. Within this aquatic environment of rapidly changing physical and chemical parameters, numerous microbial communities develop—some of which affect oxidation and mineral precipitation. Microbes are responsible for rapid oxidation of iron and arsenic in thermal outflows, and for catalyzing the production of sulfuric acid from the oxidation of elemental sulfur. The attractive visual display of colors observed in Yellowstone's geothermal waters reflects this interplay of physical, chemical, and biological phenomena.

Oxidation of dissolved sulfide to thiosulfate occurs abiotically, and thiosulfate can be found in many of Yellowstone's thermal waters—at any pH, temperature, and composition. Polythionates, on the other hand, are rarely found in Yellowstone waters but are associated with sulfur hydrolysis in Cinder Pool. Oxidation rates of iron and arsenic in overflows have been estimated at 1-3 mM/h and 0.04-0.1 mM/h, respectively—orders of magnitude faster than the abiotic rate. The abiotic production of thiosulfate from oxidation of dissolved sulfide at Angel Terrace and Ojo Caliente is about 3-30 μM/min, faster by 2-3 orders of magnitude than the laboratory rate at 25°C. The partitioning of dissolved sulfide between that volatilized to the air and that oxidized to thiosulfate has been estimated at Angel Terrace and at Ojo Caliente. For the pH range of 6-8 and the temperature range of 50-93°C, 67-86% of the dissolved sulfide is lost to the atmosphere and 10-33% is oxidized to thiosulfate. Only a very small percentage, if any, forms elemental sulfur under these conditions.



***Key Words***

arsenic
calcite
geothermal
degassing
oxidation-reduction
sulfide
thiosulfate

## 1.0 INTRODUCTION

As geothermal waters rise to the surface, they undergo rapid decreases in temperature and pressure. Water discharged by a geyser eruption decreases suddenly in pressure and temperature, and hot spring overflows decrease less suddenly. Further decreases in temperature occur as these thermal discharges flow across the ground surface to rivers and lakes. These phenomena provide a wide variety of unusual and often variegated displays that attract millions of visitors to Yellowstone National Park each year. Less well-known are the chemical and biological transformations that accompany these physical changes.

This paper presents a summary of the changes in water chemistry that occur during the outflow and cooling of water from thermal features dating back to 1974 (Ball et al. 1998a). The changes in water chemistry are caused by physical gradients, inorganic chemical reactions, and biological processes. The rates of these processes are not well known because few people have measured them, yet without this basic information there is no basis for establishing the relations among physical, chemical, and biological gradients. One of the important objectives of our research at the U.S. Geological Survey is to discern the driving forces for observed changes in aquatic chemistry. For example, are oxidation reactions dominantly biotic or abiotic? Are mineral-precipitation reactions catalyzed by co-existing microbial communities, or are microbes non-participating, chemically inert surfaces that simply increase the rate of nucleation? This paper summarizes our knowledge of the major processes of degassing, biotic and abiotic oxidation, and mineral precipitation that dominate the changing chemistry of Yellowstone's thermal water discharges based on data published in Ball et al. (1998b) and McCleskey et al. (2005).

## 2.0 MAJOR PHYSIOCHEMICAL PROCESSES

### 2.1 Hot-Water and Vapor-Dominated Systems

The dynamic chemistry of thermal discharges is related to a number of factors that begin with the hydrothermal system (rock leaching, mineral dissolution-precipitation-exchange reactions, gas reactions, boiling of fluids at depth, and mixing of thermal fluids with ground waters at shallow depths). These processes have been reviewed by Ellis and Mahon (1977), Fournier (1989, and this volume) and Henley et al. (1984) and can be summarized as water-rock interactions, boiling, and dilution.

Thermal features can be dominantly hot-water or vapor-dominated systems (Fournier this volume; White et al. 1971). Consequent to water-rock interactions, these two system types and the amount of dilution with shallow ground waters set the stage for different initial chemistries of thermal discharges.

Hot-water systems are characterized by dominance of liquid-phase flow, and carry solutes that stay in solution during boiling, such as chloride, silica, and major cations (Ca, Mg, Na, and K). Vapor-dominated systems are characterized by dominance of vapor-phase or gas flow. Fumaroles, such as Double Bulger in Norris Geyser Basin (White et al. 1988), are vapor-dominated, but even hot springs that appear to be hot-water systems can be vapor-dominated, e.g., Frying Pan Spring. The Mud Volcano area is probably the largest vapor-dominated area in Yellowstone. These features consist of hot gases that discharge into and mix with surface waters (and shallow ground waters) to create hot pools of acid water. Volatile components such as $H_2S$, $CO_2$, $NH_3$, $N_2$, Hg, and low-molecular-weight hydrocarbons (e.g., $CH_4$) are partitioned into the gas phase during boiling and affect the chemistry of vapor-dominated systems. The extent to which fluid solutes partition between vapor and liquid phases on boiling can depend on their temperature and pressure of separation as well as their initial composition. For example, arsenic normally stays in the liquid phase during steam separation at boiling near ambient pressures, but at Solfatara, in Italy's Phlegrean fields, some fumaroles at about 180°C contain volatile arsenic that coats exposed surfaces with orpiment and realgar (D.K. Nordstrom 2001, personal communication). Similarly, the amount of boron that partitions into the steam phase increases as temperature increases (Ellis and Mahon 1977). Ammonia also partitions more into the steam phase with increasing temperature (Jones 1963). Thermal features also can alternate between vapor-domination and liquid-domination depending on water-table drawdown which

can be affected by geothermal energy production, climate change, and seasonal change.

In several Yellowstone locations, hot springs of circumneutral pH are found within a few meters of a low-pH pool—e.g., Minute Geyser (pH 7.6) near Branch Spring (pH 3.9) and Perpetual Spouter (pH 6.8) near an unnamed acid spring (pH 2.7). These pairs of springs and many others are the result of steam separation, probably from the same conduit at shallow depth. The acid spring receives gas discharge with $H_2S$ enrichment that oxidizes to sulfuric acid at or near the surface, whereas the circumneutral spring contains the liquid after steam separation without $H_2S$. Both may have mixed with shallow dilute ground waters, but the acid spring will always have the lower chloride concentration and the higher sulfate concentration. Preliminary data from stable water isotopes confirm this pattern in that acid sulfate waters have consistently heavier values from evaporative concentration at or near the surface.

### 2.2 $CO_2$ Degassing

One of the dominant gases discharging in Yellowstone is $CO_2$. In high-temperature and high-pressure systems, the fugacity or partial pressure of $CO_2$ can be highly supersaturated relative to atmospheric conditions. Quite often the bubbles seen in thermal springs are not caused by water boiling but by degassing of $CO_2$, $N_2$, and smaller amounts of other gases. Degassing of $N_2$ causes no change in the discharging water chemistry, but degassing of $CO_2$ causes substantial increases in pH for waters with initial pH values that are circumneutral to basic. As $CO_2$ escapes to the atmosphere, the pH rises by consuming protons during hydrolysis as shown in the following reaction:

$$HCO_3^- + H^+ \rightarrow CO_2 \uparrow + H_2O$$

How much and how quickly the pH increases is a complex function of the initial temperature and pH, the rate of cooling, the water's flow rate, the amount of turbulence, and the water's composition. Because of the high concentrations of $CO_2$ in most geothermal waters, the carbonate chemistry usually dominates the pH buffering in other than acid waters. The increase in pH also increases the saturation state of the water with respect to calcite solubility:

$$Ca^{2+} + 2HCO_3^- \rightarrow CaCO_3 + CO_2 \uparrow + H_2O$$

Hence, calcite is more likely to precipitate in thermal waters undergoing $CO_2$ loss. A comparison of degassing at Canary Spring with degassing at Angel Terrace shows these effects quite clearly.

### 2.3 $H_2S$ Degassing and Sulfur Oxidation

The concentration of $H_2S$ is usually much smaller (a few percent or less by volume) than that of $CO_2$ (50-99% by volume, excluding $H_2O$). Consequently, sulfide hydrolysis has little effect on the pH of thermal waters. However, sulfide hydrolysis does contribute to $H_2S$ volatility which increases at low pH:

$$HS^- + H^+ \rightarrow H_2S \uparrow$$

The greater volatilization under acid conditions (pK for this first hydrolysis reaction is about 7.0 at 25°C) explains why acid hot springs are noticeably stinkier than neutral to basic hot springs with comparable amounts of $H_2S$.

Oxidation of $H_2S$ ultimately forms sulfuric acid and is the source of most acid waters in geothermal areas. However, the hydrogeological, microbiological, and geochemical processes by which acid sulfate waters are formed can be complicated. The oxidation of $H_2S$ occurs by reaction with oxygen in the atmosphere, but shallow ground waters can also carry some dissolved oxygen and that oxygen can also mix with ascending geothermal waters. Solfataras are geothermal vents that give off sulfurous gases. These gases typically contain $H_2S$ and $SO_2$, and the $H_2S$ oxidizes to elemental sulfur that does not readily oxidize so that it tends to accumulate at the surface. D.K. Nordstrom has observed elemental sulfur mounds more than a meter high on Ebeko Volcano, Kuril Islands, Russia, with gases discharging at temperatures up to 130°C. Such solfataras are common in active volcanic regions around the world. These sulfur mounds and layers are then actively oxidized by sulfur-oxidizing microbes to sulfuric acid. Also, solfataras can be buried by flows or sediments, and when they are intercepted by ascending thermal fluid, the sulfur will react with the hot water to form a variety of sulfoxyanion species (thiosulfate, polythionate, and sulfate) such as those found at Cinder Pool (Xu et al. 2000). Most of

the sulfuric acid is formed near the surface because that is where elemental sulfur accumulates. Sulfuric acid formed at the surface then becomes part of the recharge water that infiltrates back into the aquifer and mixes with ascending thermal fluids, making them more acidic over time. This concept is supported by the strong relation between the highest sulfate concentrations and the heaviest water stable isotopes, indicating high evaporation rates of the waters containing high concentrations of sulfuric acid.

The formation of sulfuric acid from $H_2S$ is achieved through a complex chain of reactions that involves both biotic and abiotic reactions. Upon exposure to low concentrations of oxygen, two reactions occur abiotically and rapidly—oxidation of dissolved sulfide to thiosulfate and to polysulfides:

$$H^+ + 2HS^- + 2O_2 \rightarrow HS_2O_3^- + H_2O$$

$$(n\text{-}1)H^+ + nHS^- + (\tfrac{n-1}{2})O_2 \rightarrow HS_n^- + (n\text{-}1)H_2O$$

The formation of thiosulfate is the more important reaction because under acid conditions polysulfides are unstable and break down to elemental sulfur and sulfide (hence they tend to be inhibited from forming), and under basic conditions the rate for polysulfide formation is substantially slower than the rate for sulfoxyanion formation. Thiosulfate is also unstable in acid solutions, but it has been measured at low pH (2.3 at Frying Pan Spring; see Ball et al. 1998b and Xu et al. 1998) and is stable at circumneutral pH (Xu and Schoonen 1995). Thiosulfate degrades in acid solutions to elemental sulfur and sulfite:

$$H^+ + S_2O_3^{2-} \rightarrow S^0 + HSO_3^-$$

and sulfite rapidly oxidizes abiotically to sulfuric acid:

$$HSO_3^- + {}^1/_2O_2 \rightarrow SO_4^{2-} + H^+$$

The elemental sulfur accumulates because of its slow reactivity with water below 100°C. Numerous microbes, however, utilize sulfur as an energy source and catalyze the oxidation of sulfur to sulfuric acid:

$$S^0 + {}^3/_2O_2 + H_2O \rightarrow SO_4^{2-} + 2H^+$$

Only this last reaction and the oxidation of thiosulfate at neutral to high pH have an essential microbial participation. The other reactions have been demonstrated to proceed rapidly in abiotic laboratory studies (Chen and Morris 1972; Giggenbach 1972; O'Brien and Birkner 1977; Zhang and Millero 1994). The formation and stability of thiosulfate in Yellowstone's thermal waters also have been demonstrated wherever dissolved sulfide occurs in the discharging thermal feature (Xu et al. 1998). A complicating geologic factor is the hydrolysis of molten sulfur when hot fluids react with a buried solfatara at temperatures greater than boiling (114°C, the melting point of sulfur), such as that found in Cinder Pool (White et al. 1988; Xu et al. 2000). The molten solfatara was discovered at 20 m depth (White et al. 1988) and observed with a high-temperature camera lens by NASA researchers (J. Trent 1999, personal communication). Sulfur hydrolysis leads to the formation of thiosulfate and polythionates even in the absence of oxygen.

### 2.4 Arsenic and Iron Oxidation

Both dissolved arsenic and dissolved iron should be in their reduced oxidation states in subsurface thermal waters, i.e., arsenite ($As^{III}O_3^{3-}$) and ferrous iron ($Fe^{2+}$). Arsenic does not oxidize abiotically when exposed to air unless a strong oxidant is present (such as permanganate, nitrate, or ferric iron), and its oxidation rate is affected substantially by pH. Ferrous iron, however, oxidizes spontaneously to ferric iron at neutral pH and precipitates insoluble hydrous ferric oxides, but the rate slows down by orders of magnitude at low pH. Hence, if iron is oxidizing rapidly in an acid water (pH<4) then microbes are likely to be catalyzing the reaction. If arsenic is oxidizing rapidly at any pH, then microbes likely are catalyzing the reaction. Reduced sulfur compounds, such as dissolved sulfide or thiosulfate, are important inhibitors to arsenic oxidation. Both sulfide and thiosulfate have been shown to reduce arsenate to arsenite (Chapin 1914; Cherry et al. 1979; DeKonnick 1909; Forbes et al. 1922; Rochette et al. 2000; see review in McCleskey et al. 2004), and their presence in thermal water may inhibit arsenite oxidation or reduce any arsenate to arsenite. This inhibiting effect can be clearly seen in **Figure 1 (next page)** of the ratio of arsenite (As III) to total dissolved arsenic relative to the concentration

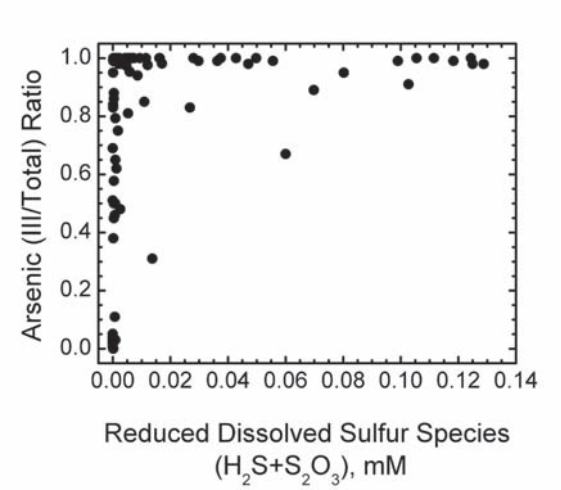


**Figure 1. Arsenic (III/total) weight ratio relative to dissolved, reduced sulfur species (sulfide plus thiosulfate) for samples from Mammoth Hot Springs and Norris, Gibbon, and Lower Geyser Basins.**

of sulfide plus thiosulfate. For concentrations of sulfide plus thiosulfate >$10^{-5}$ M, arsenic is predominantly in the reduced state. Recent research also indicates that sulfide inhibits the cellular arsenic-oxidizing mechanism in microbes (D'Imperio et al. 2005) so that a microbiological inhibition could be preventing arsenic oxidation.

The reduction of arsenate by dissolved sulfide proceeds differently from reduction by thiosulfate. Dissolved sulfide oxidizes to elemental sulfur, whereas thiosulfate oxidizes to sulfate as shown in the equations that follow. Undoubtedly these reactions are oversimplified and do not reveal the mechanisms that help to establish the kinetics.

$$HAsO_4^{2-} + HS^- + 3H^+ \rightarrow H_3AsO_3^0 + S^0 + H_2O$$

$$4HAsO_4^{2-} + S_2O_3^{2-} + H_2O + 6H^+ \rightarrow 4H_3AsO_3^0 + 2SO_4^{2-}$$

Both of these reactions proceed rapidly and abiotically at low pH, but the thiosulfate reduction of arsenate is less important because thiosulfate is unstable at low pH and arsenic is usually present in much higher concentrations than thiosulfate. Preliminary data from Ojo Caliente indicate that arsenic can oxidize in the presence of a few µM of thiosulfate. Both arsenate and thiosulfate are present at concentrations of a few µM at pH >8. Laboratory experiments may be needed to better define the reaction conditions and rates.

### 2.5 Evaporation

Thermal outflows cool from any temperature at or below the boiling point of water (about 93°C for Yellowstone's elevation) to ambient temperatures of air and ground surfaces. Cooling is caused by evaporation of the water, and because of large temperature gradients, increases in the concentrations of solutes can be measured in outflows. If the temperature decreases are measured at downstream overflow sampling locations, the amount of solute concentration increase from evaporation can be calculated from the heat capacity of water and the enthalpy of vaporization. Such checks are helpful for corroborating the analytical determinations and determining whether or not a constituent is undergoing mass transfer. Corroborations with heat-capacity calculations have shown that the agreement for chloride is well within analytical error (<3%).

### 2.6 Mineral Precipitation

In addition to calcite and sulfur precipitation mentioned previously, the precipitation of numerous other minerals and salts may occur in geothermal environments including silica, silicate clay minerals, metal sulfides, hydrous iron oxides, scorodite, and efflorescent salts including halite and gypsum.

Thermal waters contain high silica concentrations because quartz solubility increases dramatically with temperature. At temperatures of 200-400°C, dissolved silica concentrations are several hundred mg/$kg_{H2O}$, and as this water cools on the surface, it becomes greatly supersaturated with respect to silicate minerals causing them to precipitate. Silica sinter is very common as an apron surrounding many hot springs but is more commonly associated with neutral to basic hot springs because the rate of silica polymerization and precipitation is slower at low pH.

Acid-sulfate thermal waters with pH values of 1-4 are common in many Yellowstone locations. Such conditions promote the precipitation of alunite [$KAl_3(SO_4)_2(OH)_6$], and microcrystals of alunite have been found in several

mud samples collected from acid springs (S. Utsunomiya, D.K. Nordstrom, and R.B. McCleskey, unpublished TEM and SEM data). Raymahashay (1968) investigated the geochemistry of alunite formation in the Artist Paintpots of Gibbon Basin, Yellowstone, and concluded that alunite formation should be common in acid sulfate thermal waters.

Clay minerals in Yellowstone's hot spring environments have not been studied thoroughly, but in addition to silica and alunite, kaolinite also is common. Smectites, zeolites, and other clay minerals have been found, especially in drill cores, but their occurrence and distribution in surficial materials is not well known. The soil survey by Rodman et al. (1996) provides a Park-wide framework for more detailed mineralogical studies of thermal and non-thermal surficial clays.

Pyrite and some ferrous sulfide minerals have been reported in thermal waters from Yellowstone, but many of the grey-to-black waters and muds may be colored by carbonized organic matter rather than by pyrite. The inkpots at Washburn were found to contain abundant woody-type organic material blackened to carbon—the carbonizing effect caused by boiling and by sulfuric acid. Black material thought to be pyrite in hot springs from the Mud Volcano area did not contain pyrite. The cinders at Cinder Pool were found to contain about 2% pyrite and 98% sulfur, but these minerals are forming at about 20 m depth. Orpiment and realgar were first reported in Yellowstone by Weed and Pirsson (1891). Arsenic sulfides such as "amorphous orpiment" and possibly realgar have been found in the Ragged Hills and One Hundred Spring Plain areas of Norris Geyser Basin (Nordstrom et al. 2003).

Scorodite [$FeAsO_4 \cdot 2H_2O$] was reported by Hague (1887) from Josephs Coat Spring, but no confirmation has been reported using modern techniques of X-ray, electron microscopy, or microprobe. More recently, Langner et al. (2001) and Inskeep et al. (2004) have characterized low-pH (~3) Fe microbial mats in Norris Geyser Basin and shown that the primary biomineralized solid phase is an amorphous As(V)-rich hydrous ferric oxide (As:Fe mole ratios = 0.6-0.7). This phase is partly stabilized by the extremely high arsenate sorption densities that limit the number of Fe atoms in an $Fe^{III}$-OH octahedrally-coordinated cluster (see also Inskeep and McDermott, this volume).

Efflorescent salts have not been studied extensively in Yellowstone but halite and gypsum have been found in samples collected from One Hundred Spring Plain. Gypsum-like salts have been observed in hand specimens from Mammoth Hot Springs and Brimstone Basin.

## 3.0 ANALYTICAL METHODS

Temperature, Eh, pH, specific conductance, dissolved oxygen (DO), and $H_2S$ were measured on site. Measurements of Eh and pH were made on unfiltered water pumped through a flow-through cell. A mobile laboratory truck containing an ion chromatograph, ultraviolet-visible spectrophotometer, autotitrator, and reagent-grade water system was set up as close to each sampling site as feasible so that unstable intermediate sulfur oxyanion species (Moses et al. 1984), Fe(II/III) species (Stookey 1970; To et al. 1999), alkalinity, and acidity (Barringer and Johnsson 1989) could be determined as soon as possible after sample collection. Major cation and trace metal concentrations were determined by inductively coupled plasma-optical emission spectrometry (ICP-OES), and trace metal below the ICP-OES quantification limit was measured using graphite furnace-atomic absorption spectrometry. Hydride generation-atomic absorption spectrometry was used to measure total dissolved arsenic, As(T), and dissolved arsenite, As(III), concentrations (McCleskey et al. 2003). Concentrations of sulfate, chloride, and bromide were determined using ion chromatography (Brinton et al. 1995). Fluoride concentrations were determined using an ion-selective electrode (Barnard and Nordstrom 1980). Quality assurance and quality control procedures included charge imbalance calculations; analyses of standard reference water samples; analyses using multiple methods; spike recoveries; replicate analyses; and analyses of field and reagent blanks (McCleskey et al. 2005).

Chemical analyses of all thermal features discussed in this paper are shown in **Table 1 (next four pages)**. These data

**Table 1.** **Results of water analyses [---, not determined]**

| Sample code number | 00WA142 | 00WA143 | 01WA135 | 97WA123 |
|---|---|---|---|---|
| Name and/or Site Description | Minute Geyser | Branch Spring | Perpetual Spouter | Frying Pan Spring |
| Date collected | 6/24/2000 | 6/24/2000 | 9/13/2001 | 8/13/1997 |
| Temperature (°C) | 93 | 79 | 89.8 | 60.6 |
| pH, field/lab | 7.63 / 7.61 | 3.91 / 4.07 | 6.75 / 6.76 | 2.22 / 2.58 |
| Spec. cond. (µS/cm) field/lab | 1990 / 2095 | 1580 / 1662 | 2500 / 2760 | 1450 / 1851 |
| Eh (V) | --- | 0.20 | 0.011 | 0.369 |
| Density (g/mL) at 20°C | 0.9994 | 0.9993 | 0.99948 | 0.9988 |
| D.O. (mg/L) | --- | --- | --- | 0.5 |
| **Constituent (mg/L)** | | | | |
| Ca | 6.1 | 5.3 | 10.2 | 2.29 |
| Mg | 0.046 | 0.17 | 0.087 | 0.255 |
| Sr | 0.015 | 0.012 | 0.036 | 0.011 |
| Ba | 0.013 | 0.022 | 0.020 | 0.058 |
| Na | 380 | 280 | 466 | 61.2 |
| K | 34 | 30 | 55.2 | 14.6 |
| Li | 3.8 | 3.2 | 6.20 | 0.418 |
| $SO_4$ | 28 | 70 | 42.4 | 362 |
| $H_2S$ | 0.09 | 0.109 | 0.006 | 0.02 |
| $S_2O_3$ | <0.1 | 6.8 | <0.3 | --- |
| Alkalinity ($HCO_3$) | 7.8 | --- | 10.5 | --- |
| F | 4.5 | 3.4 | 6.4 | 3.43 |
| Cl | 610 | 440 | 803 | 12.1 |
| Br | 0.66 | 0.61 | 2.5 | <0.1 |
| $NO_3$ | <0.1 | <0.1 | <0.1 | <0.2 |
| $NH_4$ | 0.14 | 1.4 | <0.04 | --- |
| $SiO_2$ | 450 | 350 | 300 | 179 |
| B | 9.8 | 7.1 | 12.3 | 1.50 |
| Al | <0.08 | 0.80 | 0.14 | 4.14 |
| Fe(T) | 0.003 | 0.124 | 0.134 | 1.43 |
| Fe(II) | <0.002 | 0.124 | 0.029 | 1.41 |
| Mn | 0.018 | 0.042 | 0.046 | 0.015 |
| Cu | <0.0006 | 0.0008 | <0.0005 | <0.00005 |
| Zn | <0.001 | 0.004 | 0.001 | <0.004 |
| Cd | <0.00005 | 0.00008 | 0.0001 | 0.0001 |
| Cr | <0.0002 | 0.0002 | 0.0008 | <0.045 |
| Co | <0.001 | <0.001 | <0.0007 | <0.007 |
| Ni | <0.02 | <0.02 | <0.002 | 0.006 |
| Pb | 0.002 | 0.002 | <0.0008 | 0.002 |
| Be | 0.0006 | 0.001 | 0.002 | 0.020 |
| V | <0.001 | <0.001 | <0.002 | <0.006 |
| Se | <0.02 | <0.02 | <0.001 | <0.0003 |
| As(T) | 2.3 | 1.4 | 2.80 | 0.287 |
| As(III) | 1.1 | 1.4 | 1.06 | --- |
| Sb | <0.02 | <0.02 | 0.179 | --- |
| DOC | --- | --- | 0.5 | --- |
| Sum cations (meq/L) | 18.3 | 13.9 | 23.1 | 6.3 |
| Sum anions (meq/L) | 18.4 | 13.9 | 24.1 | 6.6 |
| Charge imbalance (percent) | -0.7 | -0.1 | -4.3 | -4.3 |

**Table 1.** Results of water analyses—continued

| Sample code number | 01WA105 | 01WA110 | 01WA118 | 01WA143 |
|---|---|---|---|---|
| Name and/or Site Description | Cinder Pool | Washburn Springs Inkpot #1 | Washburn Springs Inkpot #3 | Canary Spring |
| Date collected | 5/22/2001 | 5/23/2001 | 5/25/2001 | 9/15/2001 |
| Temperature (°C) | 91.2 | 85.0 | 71.5 | 73.0 |
| pH, field/lab | 4.32 / 3.89 | 6.39 / 7.77 | 3.71 / 3.35 | 6.50 / 7.95 |
| Spec. cond. (µS/cm) field/lab | 2090 / 2270 | 2020 / 2210 | 4070 / 4450 | 2310 / 1808 |
| Eh (V) | 0.027 | -0.154 | 0.022 | -0.123 |
| Density (g/mL) at 20°C | 0.99936 | 0.99926 | 1.00020 | 0.99924 |
| D.O. (mg/L) | --- | --- | --- | --- |
| **Constituent (mg/L)** | | | | |
| Ca | 5.23 | 22.7 | 19.3 | 342 |
| Mg | 0.021 | 8.08 | 10.0 | 75.8 |
| Sr | 0.013 | 0.178 | 0.103 | 1.89 |
| Ba | 0.019 | 0.080 | 0.012 | 0.038 |
| Na | 385 | 35.5 | 21.7 | 130 |
| K | 54.4 | 13.2 | 8.07 | 51.4 |
| Li | 4.10 | 0.034 | 0.018 | 1.53 |
| $SO_4$ | 67.0 | 774 | 1920 | 528 |
| $H_2S$ | 0.29 | 1.3 | 2.8 | 1.3 |
| $S_2O_3$ | 11 | 2.6 | <0.3 | <0.3 |
| Alkalinity ($HCO_3$) | --- | 152 | --- | 846 |
| F | 5.6 | 0.9 | 1.5 | 2.0 |
| Cl | 605 | 3.5 | 3.6 | 166 |
| Br | 0.7 | <0.1 | <0.1 | 0.6 |
| $NO_3$ | <0.1 | <0.1 | <0.1 | <0.1 |
| $NH_4$ | 5.54 | 285 | 618 | 0.99 |
| $SiO_2$ | 285 | 168 | 225 | 52.3 |
| B | 9.83 | 7.56 | 5.56 | 3.89 |
| Al | 1.38 | <0.07 | 3.31 | <0.07 |
| Fe(T) | 0.038 | 0.007 | 1.02 | 0.024 |
| Fe(II) | 0.038 | 0.007 | 1.01 | 0.023 |
| Mn | <0.001 | 0.124 | 0.286 | 0.017 |
| Cu | <0.0005 | 0.0008 | 0.0005 | 0.0012 |
| Zn | 0.004 | <0.001 | 0.012 | 0.002 |
| Cd | 0.0002 | <0.0001 | <0.0001 | <0.0001 |
| Cr | <0.0005 | <0.0005 | 0.0077 | <0.0005 |
| Co | <0.0007 | 0.0008 | <0.0007 | <0.0007 |
| Ni | <0.002 | <0.002 | 0.004 | <0.002 |
| Pb | 0.0009 | <0.0008 | <0.0008 | <0.0008 |
| Be | <0.001 | <0.001 | 0.001 | 0.002 |
| V | <0.002 | <0.002 | 0.013 | <0.002 |
| Se | <0.001 | <0.001 | <0.001 | 0.003 |
| As(T) | 2.41 | 0.0008 | 0.0002 | 0.466 |
| As(III) | 2.23 | 0.0005 | <0.0005 | 0.466 |
| Sb | 0.080 | 0.001 | 0.002 | 0.003 |
| DOC | --- | 4.1 | 2.9 | 2.1 |
| Sum cations (meq/L) | 19.3 | 17.4 | 33.9 | 24.9 |
| Sum anions (meq/L) | 18.6 | 17.2 | 35.7 | 24.0 |
| Charge imbalance (percent) | 4.1 | 1.0 | -5.2 | 3.8 |

**Table 1.** **Results of water analyses—continued**

| Sample code number | 01WA144 | 94WA120 | 94WA123 | 94WA100 |
|---|---|---|---|---|
| Name and/or Site Description | Canary Spring - near base of travertine terrace above wetland area | Angel Terrace (source) | Angel Terrace (down drainage) | Ojo Caliente Spring (source) |
| Date collected | 9/15/2001 | 6/30/1994 | 6/30/1994 | 6/28/1994 |
| Temperature (°C) | 38.5 | 71.4 | 56.5 | 93 |
| pH, field/lab | 8.13 / 8.03 | 6.43 / 8.47 | 7.52 / 8.32 | 7.72 / 8.61 |
| Spec. cond. (µS/cm) field/lab | 2030 / 1839 | 2170 / 2340 | 2245 / 1810 | 1517 / 1595 |
| Eh (V) | 0.096 | -0.041 | 0.178 | -0.156 |
| Density (g/mL) at 20°C | 0.99926 | 1.00013 | 0.99975 | 0.99936 |
| D.O. (mg/L) | --- | 0.5 | 2.9 | 0.1 |
| **Constituent (mg/L)** | | | | |
| Ca | 206 | 320 | 270 | 1 |
| Mg | 82.3 | 74.8 | 72.9 | 0.001 |
| Sr | 0.970 | 1.63 | 1.31 | 0.008 |
| Ba | 0.026 | <0.1 | <0.1 | <0.04 |
| Na | 137 | 136 | 132 | 331 |
| K | 53.8 | 57.4 | 53.6 | 9.5 |
| Li | 1.67 | 1.64 | 1.67 | 3.96 |
| $SO_4$ | 565 | 547 | 557 | 20.7 |
| $H_2S$ | <0.002 | 3.01 | 0.09 | 1.09 |
| $S_2O_3$ | <0.3 | <0.09 | 0.553 | 0.3 |
| Alkalinity ($HCO_3$) | 362 | 734 | 634 | 232 |
| F | 1.2 | 2.9 | 2.0 | 31.6 |
| Cl | 177 | 165.0 | 170.0 | 324 |
| Br | 0.6 | 0.554 | 0.573 | 1.2 |
| $NO_3$ | 0.2 | 0.034 | <0.031 | 0.1 |
| $NH_4$ | <0.3 | 0.91 | 0.88 | 0.089 |
| $SiO_2$ | 55.9 | 54 | 54 | 243 |
| B | 4.16 | 3.56 | 3.48 | 3.98 |
| Al | <0.07 | 0.01 | 0.01 | 0.28 |
| Fe(T) | <0.002 | 0.0297 | 0.0025 | 0.023 |
| Fe(II) | <0.002 | 0.0297 | 0.0025 | 0.023 |
| Mn | 0.014 | <0.3 | <0.3 | <0.12 |
| Cu | <0.0005 | <0.35 | <0.35 | <0.14 |
| Zn | 0.002 | <0.025 | <0.025 | <0.01 |
| Cd | <0.0001 | <0.1 | <0.1 | <0.04 |
| Cr | <0.0005 | <0.225 | <0.225 | <0.09 |
| Co | <0.0007 | <0.1 | <0.1 | <0.04 |
| Ni | <0.002 | <0.1 | <0.1 | <0.04 |
| Pb | <0.0008 | <0.375 | <0.375 | <0.15 |
| Be | <0.001 | <0.001 | <0.001 | <0.001 |
| V | <0.002 | <0.05 | <0.05 | <0.02 |
| Se | 0.001 | --- | --- | --- |
| As(T) | 0.539 | 0.47 | 0.62 | 0.86 |
| As(III) | 0.375 | --- | --- | --- |
| Sb | 0.003 | --- | --- | --- |
| DOC | 1.1 | 1.1 | --- | 1 |
| Sum cations (meq/L) | 20.3 | 24.3 | 21.7 | 14.6 |
| Sum anions (meq/L) | 18.4 | 22.5 | 21.6 | 14.9 |
| Charge imbalance (percent) | 9.8 | 7.5 | 0.5 | -1.8 |

**Table 1.** **Results of water analyses—continued**

| Sample code number | 94WA110 | 01WA103 | 01WA104 |
|---|---|---|---|
| Name and/or Site Description | Ojo Caliente (down drainage) | Nymph Creek Spring (source) | Nymph Creek (32 meters from source) |
| Date collected | 6/29/1994 | 5/21/2001 | 5/21/2001 |
| Temperature (°C) | 66.6 | 59.3 | 47.0 |
| pH, field/lab | 8.21 / 8.73 | 2.93 / 2.87 | --- / 2.88 |
| Spec. cond. (µS/cm) field/lab | 1628 / 1647 | 950 / 1222 | 1060 / 1216 |
| Eh (V) | 0.195 | 0.346 | 0.229 |
| Density (g/mL) at 20°C | 0.99935 | 0.99881 | 0.99871 |
| D.O. (mg/L) | 2.7 | <0.05 | <4.1 |
| **Constituent (mg/L)** | | | |
| Ca | 1.01 | 6.76 | 7.01 |
| Mg | 0.01 | 2.28 | 2.34 |
| Sr | 0.006 | 0.016 | 0.016 |
| Ba | <0.04 | 0.032 | 0.031 |
| Na | 342 | 67.4 | 71.2 |
| K | 9.9 | 42.5 | 45.9 |
| Li | 4.13 | 0.109 | 0.130 |
| $SO_4$ | 22.5 | 278 | 280 |
| $H_2S$ | 0.06 | 0.066 | <0.002 |
| $S_2O_3$ | 0.589 | <0.3 | <0.3 |
| Alkalinity ($HCO_3$) | 244.1 | --- | --- |
| F | 33.1 | 0.6 | 0.6 |
| Cl | 335.0 | 36.2 | 33.9 |
| Br | 1.24 | <0.1 | <0.1 |
| $NO_3$ | <0.031 | <0.1 | <0.1 |
| $NH_4$ | 0.0130 | 0.99 | 0.91 |
| $SiO_2$ | 257 | 251 | 231 |
| B | 4.02 | 0.70 | 0.69 |
| Al | 0.28 | 2.34 | 2.42 |
| Fe(T) | 0.0007 | 2.30 | 2.09 |
| Fe(II) | 0.0007 | 2.19 | 0.746 |
| Mn | <0.12 | 0.107 | 0.111 |
| Cu | <0.14 | <0.0005 | <0.0005 |
| Zn | <0.01 | 0.024 | 0.025 |
| Cd | <0.04 | 0.0001 | 0.0001 |
| Cr | <0.09 | 0.0044 | 0.0042 |
| Co | <0.04 | <0.0007 | <0.0007 |
| Ni | <0.04 | <0.002 | <0.002 |
| Pb | <0.15 | <0.0008 | <0.0008 |
| Be | <0.001 | 0.001 | 0.002 |
| V | <0.02 | <0.002 | <0.002 |
| Se | --- | <0.001 | <0.001 |
| As(T) | 1.44 | 0.086 | 0.0811 |
| As(III) | --- | 0.0753 | 0.0101 |
| Sb | --- | 0.003 | 0.002 |
| DOC | 1.1 | --- | --- |
| Sum cations (meq/L) | 15.7 | 6.0 | 6.4 |
| Sum anions (meq/L) | 15.5 | 6.1 | 6.1 |
| Charge imbalance (percent) | 1.2 | -2.5 | 3.9 |

**Figure 2. Photograph of Canary Spring at its discharge point on September 15, 2001**

**Figure 3. Photograph of Canary Spring overflow on September 15, 2001.**

are extracted from U.S. Geological Survey Reports (Ball et al. 1998a, 1998b; McCleskey et al. 2005). Further descriptions of sampling and analytical techniques can be found in these reports.

## 4.0 EXAMPLES OF THERMAL OVERFLOWS

### 4.1 Canary Spring, Mammoth Hot Springs

Canary Spring has flowed continuously for long periods of time along the south side of the Mammoth Hot Springs terraces. Its main discharge point frequently moves because of cementation by calcite precipitation and bacterial growth.

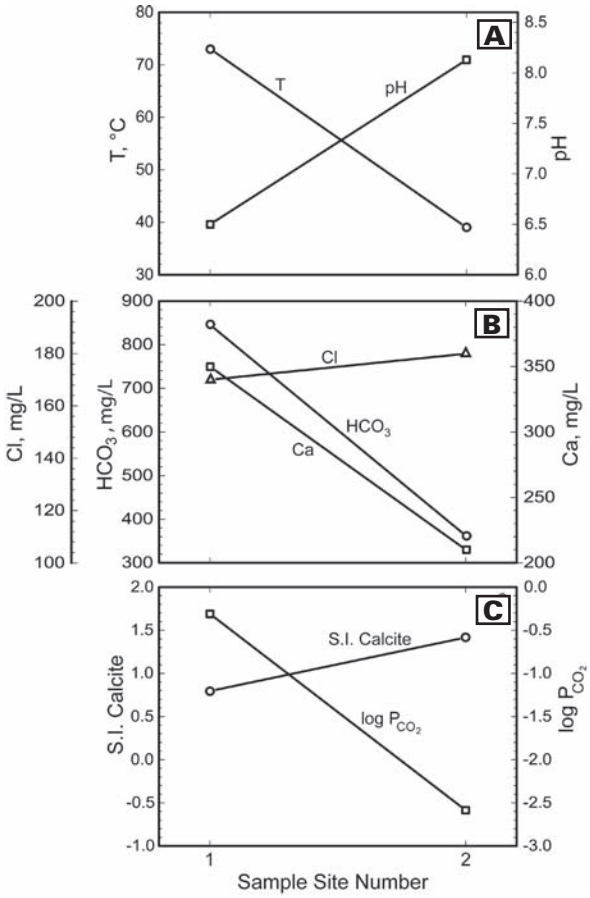


**Figure 4. Plots for Canary Spring showing changes from point of discharge to base of terrace in: A.** Temperature and pH; **B.** Calcium, bicarbonate, and chloride concentrations; and **C.** Saturation index (SI) for calcite and log $P_{CO_2}$.

Analyses of this spring water provide good examples of the processes forming travertine terraces. In September 2001 a sample was collected from near the Canary Spring discharge point (**Figure 2**), and 2 hours later another sample was collected at the base of Mammoth terraces (**Figure 3**) before the water entered a wetlands area and mixed with surface waters. No other waters were seen to mix with the water coming from Canary Spring so that the water sampled at the bottom should be the same as that issuing from the top of the terrace. The temperature decrease was about 35°C and the pH increased by more than 1.5 units (**Figure 4A**).

**Figure 4B** shows the change in the major ions (Ca, Cl, and $HCO_3$) during the several seconds that it took the water to cascade down the steep terrace slope. Chloride increased from 166 mg/L to 177 mg/L from top to bottom, and this increase agrees exactly with the chloride concentration change calculated thermodynamically from water loss on evaporation. Calcium and bicarbonate concentrations, however, decreased by larger amounts as expected if calcite is actively precipitating and $CO_2$ is degassing (in some settings $CO_2$ is taken up by photosynthetic microorganisms). **Figure 4B** illustrates the differences that can be observed between conservative and reactive solution components.

Discharge, velocity, and distance were not measured, but if an estimated 1 L/s were discharging from Canary Spring, the amount of calcite precipitating from this one spring would equal about 33 metric tons/yr. Using an average total discharge of 45 L/s from Mammoth based on the estimate of Allen and Day (1935), 1490 metric tons/yr of travertine would deposit. Sorey (1991) estimates a total discharge of 590 L/s but only 10%, or 59 L/s, erupts at the surface. This estimate is very close to that of Allen and Day (1935). Bargar (1978) states the age for Mammoth travertine must be greater than 50,000 years, and the age date of Rosholt (1976) would put it at 63,000 years. Sturchio (1990) and Sturchio et al. (1994) found ages ranging from 8,000 years at Mammoth Hot Springs to about 375,000 years at Terrace Mountain (the ridge crest above Mammoth Hot Springs).

Hot spring flow and travertine deposition appear not to be constant over this time period, but if we assume constant flow for 63,000-375,000 years, then a total of 94-560 million metric tons of travertine may have been deposited. If half the density of calcite is used (to account for the porosity in the travertine), the volume would be about 70 million to 416 million $m^3$. The only independent check of this estimate comes from estimates of calcite deposition averaging 21 cm/yr (Allen 1934) or 13.2-79 km over a 63,000-375,000 year period. If an average travertine depth of 50 m is assumed (Sturchio et al. 1994), then the area covered by the travertine would be about 1-6 $km^2$. Compared to the mapped area (Bargar 1978), the larger area is more reasonable. Flow rates were probably higher in earlier times of the Holocene than present, but considering the uncertainties in the assumptions, these estimates are not unreasonable. (More details on Mammoth Hot Springs geochemistry and microbiology can be found in Fouke et al. 2000, and this volume).

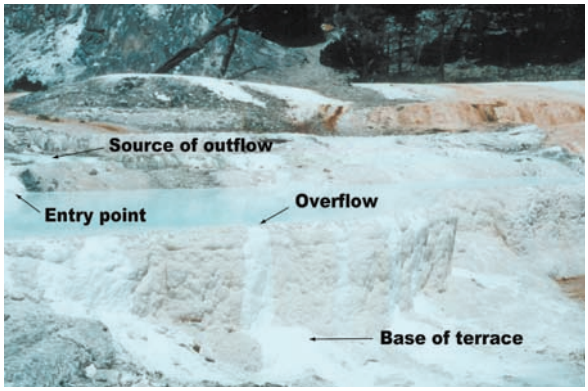


**Figure 5. Photograph of an overflow at Angel Terrace showing the four water sampling points on June 30, 1994.**

Canary Spring water discharges in a state of calcite supersaturation and large $P_{CO_2}$ supersaturation relative to atmospheric conditions (**Figure 4C**, based on data from McCleskey et al. 2005). After the loss of $CO_2$ by 2.5 orders of magnitude, the saturation index (SI) rises even higher to nearly 1.5 orders of magnitude above saturation because of the increase in pH. This amount of calcite supersaturation seems to be an upper limit based on similar results from Herman and Lorah (1987, 1988) for a calcite-precipitating spring in Virginia, and from Barnes (1965) for a calcite-depositing spring in California.

### 4.2 Angel Terrace, Mammoth Hot Springs

A similar change in water chemistry can be seen for a transect at Angel Terrace that was measured in June 1994. In this location, water flowed out of an orifice, immediately dropped over a 1-m precipice into a pool about 3 m across and then flowed over the edge of the pool (**Figure 5**). Samples were collected at the orifice, at the edge of the pool directly below the discharging fluid, at the other end of the pool next to the overflow point, and after another vertical drop from the edge of the pool (base of terrace). **Figure 6A (next page)** shows the change in temperature, pH, and dissolved oxygen across the transect. Again, a large increase in pH and dissolved oxygen accompanies the temperature decrease.

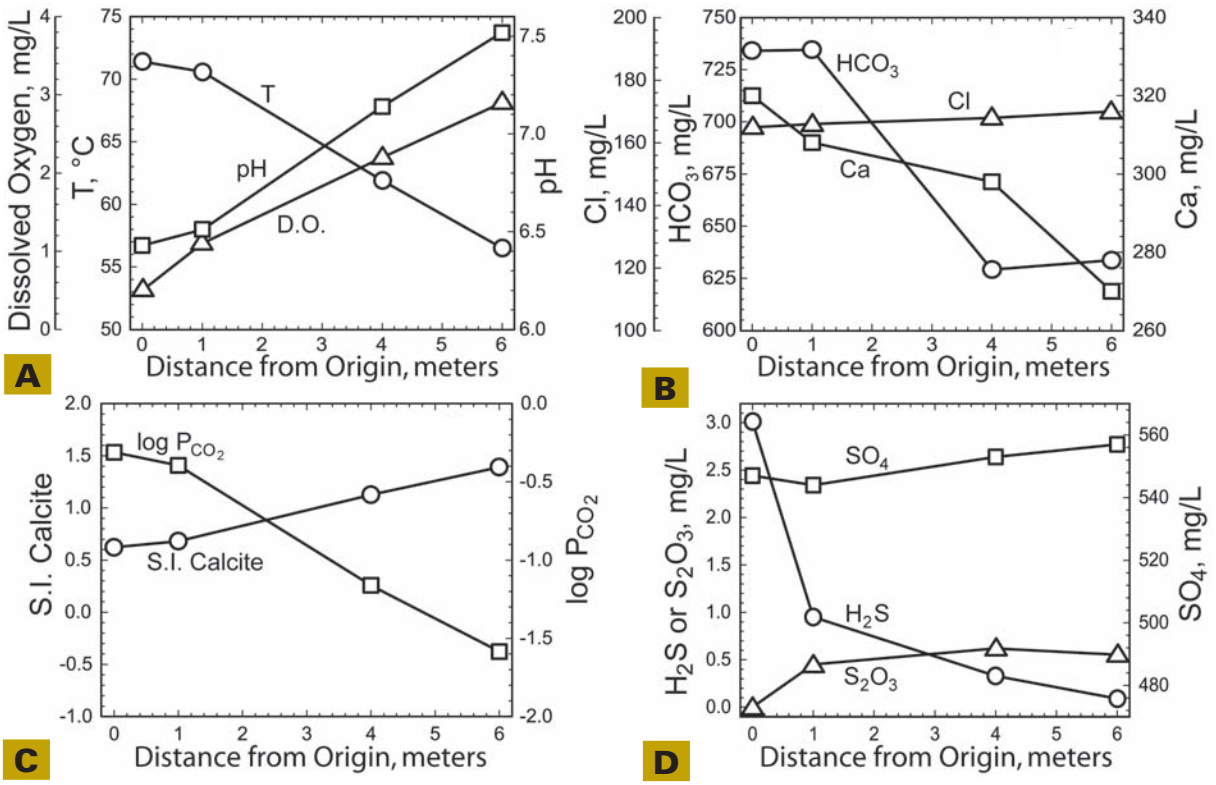


**Figure 6. Plots along an Angel Terrace overflow transect from outflowing thermal spring water into and across the pool and down from the edge of the pool.** Plots include **A.** Temperature, pH, and dissolved oxygen (DO); **B.** decreases in calcium and bicarbonate concentrations, and increase in chloride concentration; **C.** SI for calcite and log $P_{CO_2}$; and **D.** Dissolved sulfur species (0 m is from the point of outflow; the 1-m point is the distance from the outflow to near the edge of the pool; the 4-m point is the 3-m distance across the pool plus distance of vertical drop from outflow; and 6 m is after a 2-m drop from the far edge of the pool).

**Figure 6B** shows the increase in chloride concentration and the decrease in calcium and bicarbonate concentrations across this transect. The thermodynamic calculation for chloride increase on evaporation agrees with the measured value for the difference between the beginning and end points. The same trend as that of Canary Spring is apparent at Angel Terrace but is not as pronounced because the flow conditions are not turbulent and the temperature change is not as great. More calcite precipitates in the vertical falls than in the pool itself.

**Figure 6C** shows the change in SI (see Langmuir 1997 or Nordstrom and Munoz 1994) for calcite and log $P_{CO_2}$ for the Angel Terrace transect. Again the SI for calcite does not exceed 1.5 orders of magnitude and the $P_{CO_2}$ decreases by more than an order of magnitude.

Sulfur species were determined for the Angel Terrace transect and are plotted in **Figure 6D**. Sulfate concentration increases slightly from evaporation but the increase is less than the amount calculated thermodynamically. Some sulfate probably is taken up by the precipitating calcite. Dissolved sulfide concentrations begin at 3 mg/L in the source water but quickly decrease to below 1 mg/L. Thiosulfate concentrations are below detection (<0.1 mg/L) in the source water but quickly increase to 0.5 mg/L after

the first meter. No polythionates or sulfite were detected in these waters. This profile for sulfur species demonstrates the formation of thiosulfate from dissolved sulfide upon reaction with oxygen introduced by contact with air. Most of the thiosulfate is formed in the first 1 m vertical drop before the water enters the pool.

Another simple calculation provides an estimate of the fate of the dissolved sulfide in these waters. Of the original 88 μM dissolved sulfide concentration, only about 9 μM were oxidized to thiosulfate, and about 3 μM remained in solution. Hence, about 76 μM, or 86%, must have been lost to the air by volatilization. Most of the oxidation of sulfide to thiosulfate occurred in the first meter of transport which took no more than 1 second to travel 1 m down a nearly vertical waterfall. That gives a thiosulfate formation rate of about 30 μM/min.

### 4.3 Ojo Caliente, Lower Geyser Basin

In Yellowstone's Lower Geyser Basin, the flowing hot spring Ojo Caliente (**Figure 7**) has not changed substantially in chemistry for over 100 years—since the first analyses were reported by Gooch and Whitfield (1888). In September 1994, two channels were sampled: one (**Figure 8A**) contained the shortest length and fastest flow of about four discernible channels, and the other (**Figure 8B**) contained the longest length and slowest flow. The two channels diverged from a single-flow channel at about 11 m from the point of discharge. The temperature and pH profiles for these two transects are shown in **Figures 9A and 9B (next page)**.

**Figures 9C and 9D** show the transect profiles for chloride and fluoride concentrations. Thermodynamic calculations indicate steam loss accounts for the increases in concentration for both chloride and fluoride.

The transect profiles for dissolved oxygen and dissolved sulfide are shown in **Figures 10A and 10B (page 89)**. Both rapid uptake of oxygen, and rapid loss of sulfide, are apparent from these profiles. The slow-flowing transect takes up more oxygen and loses more sulfide than the fast-flowing transect as expected from the temperature profiles.

**Figure 7. Photograph of Ojo Caliente Spring at the point of upwelling water.**

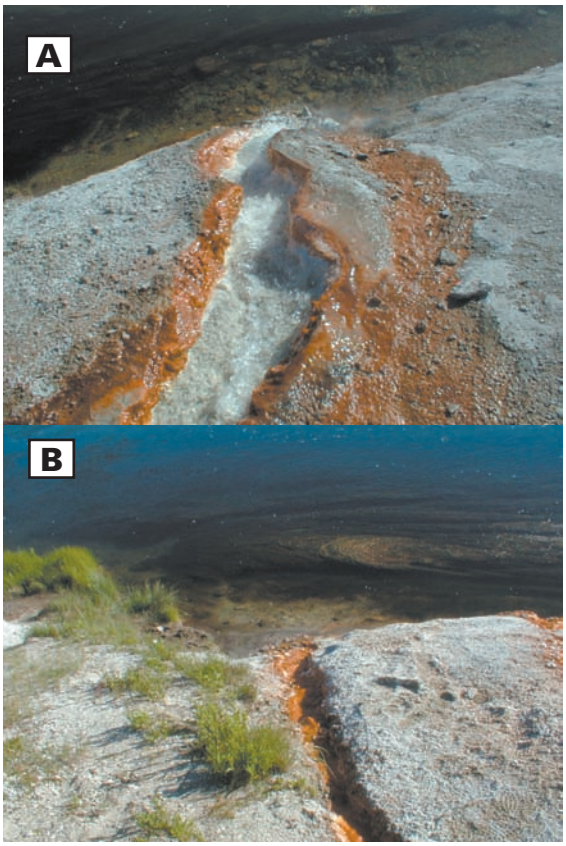


**Figure 8. A.** Photograph of the fast-flowing channel of Ojo Caliente Spring discharging into the Firehole River. **B.** Photograph of the slow-flowing channel of Ojo Caliente Spring discharging into the Firehole River.

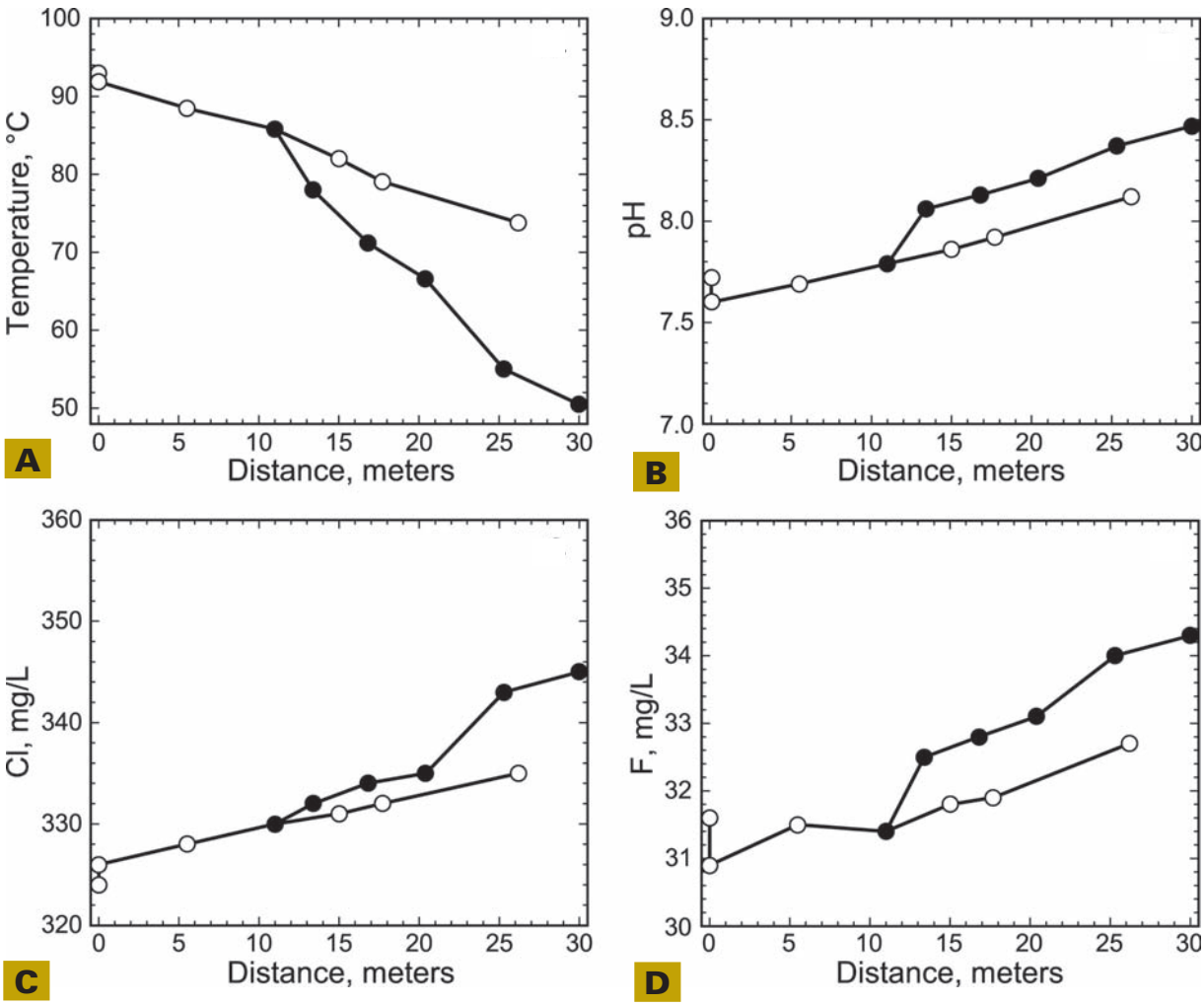


**Figure 9. Transects of: A.** temperature; **B.** pH; **C.** chloride concentrations; and **D.** fluoride concentrations from Ojo Caliente overflows that diverge at 11 m from the original source (filled circles represent slowest flowing channel and open circles represent fastest flowing channel; two additional channels of intermediate flow were not measured).

The transect profiles for thiosulfate and sulfate are shown in **Figures 10C and 10D**. Thiosulfate concentrations increase to a maximum of 5-6 µM and remain constant after about 15 m because the source of the thiosulfate (sulfide) is nearly gone. The increase in sulfate concentration is adequately accounted for by evaporation. A calculation similar to that performed for Angel Terrace results in about 67% loss of the original sulfide to the atmosphere and about 33% oxidation to thiosulfate. The lower amount of volatilization is related to the higher pH of Ojo Caliente (7.5-8.5) compared to that of Angel Terrace (6.5-7.5). These results suggest that the amount of $H_2S$ volatilization is highly sensitive to the pH of the water and not as sensitive to the temperature of the spring (Ojo Caliente is 20°C hotter than Angel Terrace yet volatilizes less sulfide). The other surprising result is that the estimate of thiosulfate formation for Ojo Caliente (about 2.7 µM/min) is nearly two orders of magnitude faster than the rate determined in

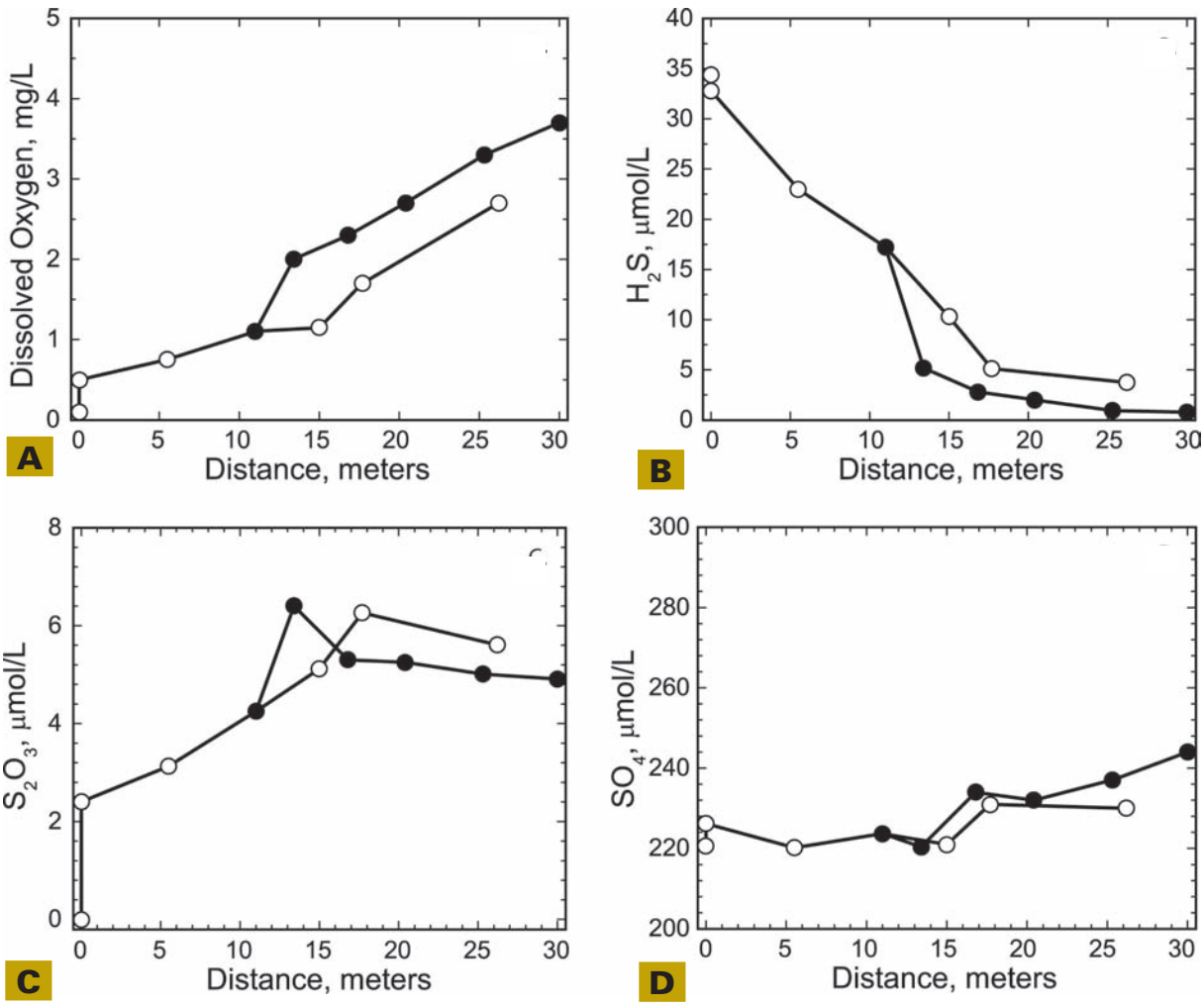


**Figure 10. Transects for: A.** dissolved oxygen; **B.** $H_2S$; **C.** thiosulfate; and **D.**sulfate concentrations in two Ojo Caliente overflow channels (filled circles represent slowest flowing water and open circles represent fastest flowing water).

laboratory studies at 25°C (about 0.05 µM/min). Although thiosulfate formation could be catalyzed by bacteria, it is also possible that the higher temperatures are responsible for the increased reaction rate. There is certainly enough oxygen present to allow the reaction to proceed.

### 4.4 Nymph Creek

Nymph Creek (**Figure 11, next page**) originates as a small thermal spring noted for its deep-green color—attributed to the growth of acid-tolerant thermophilic red algae (within the family Cyanidiales) at temperatures from 38-52°C. Recent evidence suggests that several genera within this family, including *Cyanidium*, *Cyanidioschyzon*, and *Galdieria*, may be important in acid geothermal systems (Ciniglia et al. 2004) such as Nymph Creek. There are two or three source locations for the spring, but most of the water flows from an area containing a silica sinter ledge at temperatures of 60-62°C and a pH near 2.7. This spring contains both dissolved ferrous iron (2.3 mg/L) and dissolved arsenite (0.086 mg/L).

Both iron and arsenic oxidize rapidly within a relatively short distance down drainage. Under these acid conditions, the rapid oxidation of Fe(II) is caused by microbial catalysis. The oxidation of arsenite, however, could proceed microbially or by oxidation via ferric iron. Because ferric iron oxidation of arsenite is sensitive to sunlight (sunlight substantially enhances iron photoreduction), the oxidation profile for Nymph Creek was done in daylight and then repeated at night. The four transect profiles are shown in **Figure 12** (two for ferrous iron and arsenite oxidation by day, and two for night). There is very little difference between day and night profiles, suggesting that microbes, not abiotic reactions, are responsible for arsenic oxidation. Laboratory tests to determine the rate of arsenite oxidation by ferric iron using the same water, demonstrated that the abiotic rate was much slower than the field rate at 50°C. Several microorganisms detected in the outflow channels of acid-sulfate-chloride springs are phylogenetically related to known $Fe^{II}$ and $As^{III}$ oxidizing organisms, and efforts to cultivate these organisms are still underway (Inskeep and McDermott, this volume). In some environments the same populations may be oxidizing both $Fe^{II}$ and $As^{III}$ (Jackson et al. 2001; Macur et al. 2004; Morin et al. 2003). Several other studies (Donohoe-Christiansen et al. 2004; Gihring et al. 2001; Langner et al. 2001; Wilkie and Hering 1998) have shown that arsenic-oxidizing microbes seem to be common in thermal waters. Furthermore, the rate of arsenic oxidation at Nymph Creek is at least 7 orders of magnitude faster than the inorganic rate (Nordstrom 2003). Oxidation rates for both iron and arsenic were measured once in 2001 and once in 2002. Arsenic oxidation ranged from 0.04 to 0.1 mM/hr and iron oxidation ranged from 1 to 3 mM/hr.

## 5.0 SUMMARY

Thermal equilibration of hot effluent waters is accompanied by evaporation which results in increases in concentrations of solution components, provided that their concentrations are not subject to solubility control. Concentrations of conservative components such as chloride and sulfate can be predicted with reasonable accuracy by applying thermodynamic calculations to the initial water compositions

**Figure 11. Photograph of Nymph Creek on June 28, 2002.** Red flags denote sampling sites.

The chemistry of thermal outflows in Yellowstone Park was studied in terms of carbon dioxide, oxygen, and hydrogen sulfide gas exchange; mineral precipitation; evaporative cooling; and biotic and abiotic sulfur, iron, and arsenic oxidation. In studies of two sources of Mammoth Hot Springs thermal water, degassing of carbon dioxide caused substantial changes in water chemistry, with the rate and extent of change dependent on the initial temperature and pH, cooling rate, flow rate, turbulence, and composition of the discharging water. The primary chemical change in waters of circumneutral pH upon carbon dioxide degassing is increasing pH, which can result in supersaturation and subsequent precipitation of calcite. Quartz solubility is a strong function of temperature, and near-boiling to

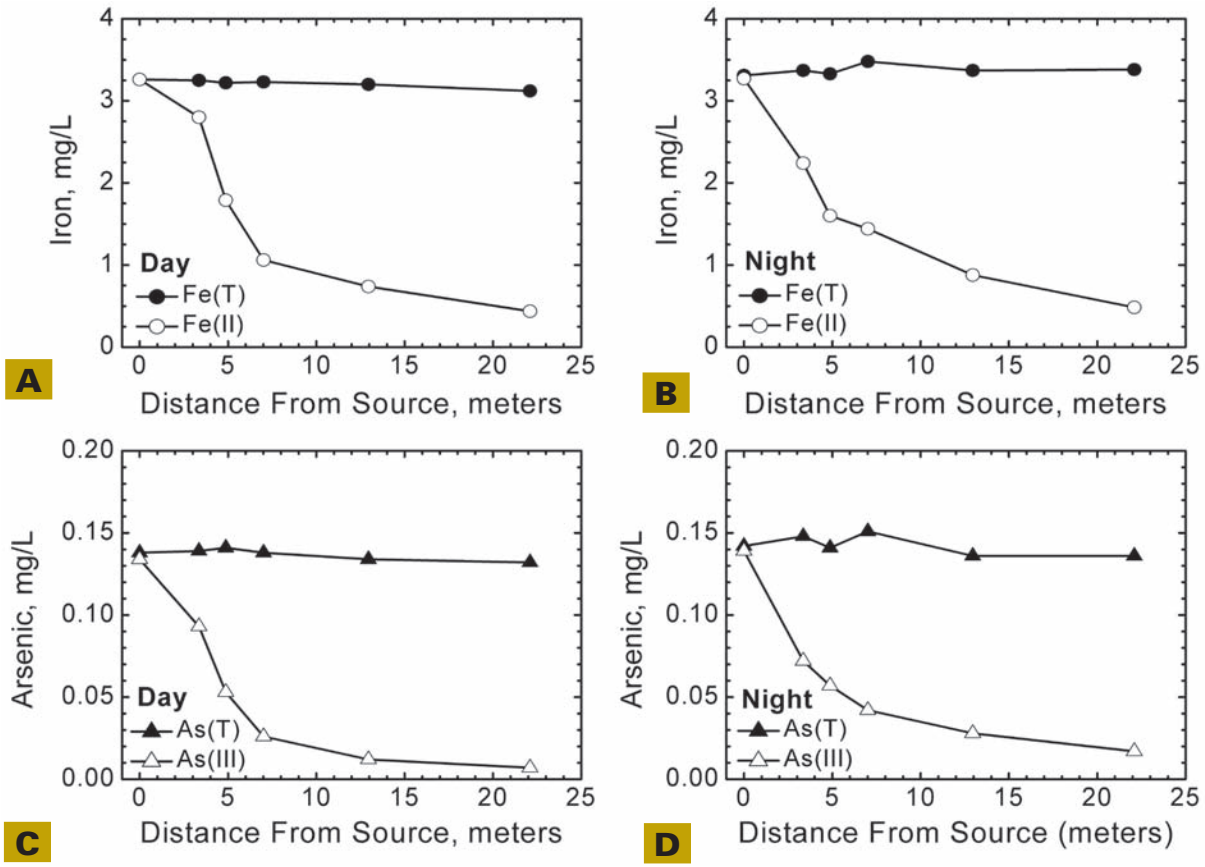


**Figure 12.** **Transects for ferrous and total dissolved iron, and arsenite and total dissolved arsenic, in Nymph Creek by day (A and C) and by night (B and D).**

boiling thermal outflows may contain several hundred mg/$kg_{H_2O}$ of dissolved silica. Silica sinter aprons are common around discharging thermal features, but less so around acidic outflows because the rate of silica polymerization and precipitation is slower at low pH.

Hydrogen sulfide usually is present in thermal waters at much lower concentrations than carbon dioxide. At pH values in the acidic range (<7) the predominant form of sulfide is $H_2S$, which can undergo either volatilization to the atmosphere or oxidation to thiosulfate and polysulfides. Formation of thiosulfate predominates over polysulfide formation because thiosulfate is more stable than polysulfides (no detectable polysulfides could be observed in our samples). Of these two reaction pathways for removal of hydrogen sulfide from solution and at 6<pH<8, 67-86% of dissolved sulfide was lost to the atmosphere by degassing, while 10-33% oxidized to thiosulfate. Greater amounts of sulfide were lost to volatilization and oxidation at lower pH values, and thiosulfate eventually is oxidized to sulfuric acid.

Arsenic oxidizes by microbial catalysis in geothermal waters. At pH values near neutral, ferrous iron oxidizes spontaneously and abiotically to ferric iron, which rapidly hydrolyzes and precipitates hydrous ferric oxide. Conversely, at acidic pH values the abiotic oxidation rate of ferrous iron is slower by several orders of magnitude, thus rapid ferrous iron oxidation at low pH implies microbial catalysis. Studies of iron and arsenic oxidation

rates at Nymph Creek during the day and at night yielded remarkably similar results, confirming that oxidation of iron and arsenic must be microbially catalyzed. Although the rate of ferrous iron oxidation can be enhanced by sunlight, no evidence for photocatalysis was detected at Nymph Creek.

## ACKNOWLEDGMENTS

*We wish to thank the National Park Service, especially all those at the Mammoth headquarters who have been so helpful on a variety of issues, but most especially John Varley, Rick Hutchinson, Ann Deutsch, Christie Hendrix, Hank Heasler, Ann Rodman, Lee Whittlesey, and Steve Miller. We thank the National Research Program of the USGS, which has funded 98% of this work. The other 2% was funded by a grant from the USEPA to investigate thioarsenites in geothermal waters. We are grateful for the thoughtful and careful review of Bill Inskeep and JoAnn Holloway. We are also indebted to those who have helped us sample at Yellowstone, including Sara LoVetere, JoAnn Holloway, Maria Hernendez, Philip Verplanck, and Britta Planer-Friedrich.*

## REFERENCES

Allen, E.T. 1934. The agency of algae in the deposition of travertine and silica from thermal waters. *Am J Sci* 28:373-89.

Allen, E.T., and A.L. Day. 1935. Hot springs of the Yellowstone National Park. *Carnegie Inst Washington Pub 466.*

Ball, J.W., D.K. Nordstrom, E.A. Jenne, and D.V. Vivit. 1998a. Chemical analyses of hot springs, pools, geysers, and surface waters from Yellowstone National Park, Wyoming and vicinity, 1974-1975. *US Geol Surv Open-File Rep* 98-182.

Ball, J.W., D.K. Nordstrom, K.M. Cunningham, M.A.A. Schoonen, Y. Xu and J.M. DeMonge. 1998b. Water-chemistry and on-site sulfur-speciation data for selected springs in Yellowstone National Park, Wyoming, 1994-1995. *US Geol Surv Open-File Rep* 98-574.

Bargar, K.E. 1978. Geology and thermal history of Mammoth Hot Springs, Yellowstone National Park, Wyoming. *US Geol Surv Bull* 1444.

Barnard, W.R., and D.K. Nordstrom. 1980. Fluoride in precipitation-I. Methodology with the fluoride-selective electrode. *Atmos Environ* 16:99-103.

Barnes, I. 1965. Geochemistry of Birch Creek, Inyo County, California a travertine depositing creek in an arid climate. *Geochim Cosmochim Acta* 29:85-112.

Barringer, J.L., and P.A. Johnsson. 1989. Theoretical considerations and a simple method for measuring alkalinity and acidity in low-pH waters by Gran titration. *US Geol Surv Water-Resources Investigations Rep* 89-4029.

Brinton, T.I., R.C. Antweiler, and H.E. Taylor. 1995. Method for the determination of dissolved chloride, nitrate, and sulfate in natural water using ion chromatography. *US Geol Surv Open-File Rep* 95-426A.

Chapin, R.M. 1914. The reduction of arsenic acid to arsenious acid by thiosulfuric acid. *J Agr Res* 1:515-17.

Chen, K.Y., and J.C. Morris. 1972. Kinetics of oxidation of aqueous sulfide by $O_2$. *Environ Sci Technol* 6:529-37.

Cherry, J.A., A.U. Shaikh, D.E. Tallman, and R.V. Nicholson. 1979. Arsenic species as an indicator of redox conditions in groundwater. *J Hydrol* 43:373-92.

Ciniglia, C., H.-S. Yoon, A. Pollio, G. Pinto, and D. Bhattacharya. 2004. Hidden biodiversity of the extremophilic Cyanidiales red algae. *Mol Ecol* 13:1827-38.

DeKonnick, L.L. 1909. The precipitation of arsenic with hydrogen sulphide. *Bull Soc Belg Chim* 23:88-94.

D'Imperio, S., C. Lehr, and T.R. McDermott. 2005. Microbial interactions with sulfide and arsenite in an acidic geothermal spring in Yellowstone National Park. Abstract A227, 15th Ann. Goldschmidt Conference.

Donohoe-Christiansen, J.S., S. D'Imperio, C.R. Jackson, W.P. Inskeep, and T.R. McDermott. 2004. An arsenite-oxidizing *Hydrogeno-*

*baculum* isolated from an acid-sulfate geothermal spring in Yellowstone National Park. *Appl Environ Microbiol* 70:1865-8.

Ellis, A.J., and W.A.J. Mahon 1977. *Chemistry and Geothermal Systems*. New York: Academic Press.

Forbes, G.S., H.W. Estil, and O.J. Walker. 1922. Induction periods in reactions between thiosulfate and arsenite or arsenate: a useful clock reaction. *J Am Chem Soc* 44:97-102.

Fouke, B.W., J.D. Farmer, D.J. Des Marais, L. Pratt, N.C. Sturchio, P.C. Burns, and M.K. Discipulo. 2000. Depositional facies and aqueous-solid geochemistry of travertine-depositing hot springs (Angel Terrace, Mammoth Hot Springs, Yellowstone National Park, U.S.A.). *J Sediment Res* 70:565-85.

Fournier, R.O. 1989. Geochemistry and dynamics of the Yellowstone National Park hydrothermal system. *Ann Rev Earth Planet Sci* 17:13-53.

Gihring, T.M., G.K. Druschel, R.B. McCleskey, R.J. Hamers, and J.F. Banfield. 2001. Rapid arsenite oxidation by *Thermus aquaticus* and *Thermus thermophilus*: field and laboratory investigation. *Environ Sci Technol* 35:3857-62.

Giggenbach, W. 1972. Optical spectra and equilibrium distribution of polysulfide ions in aqueous solution at 20°. *Inorg Chem* 11:1201-7.

Gooch, F.A., and J.E. Whitfield. 1888. Analyses of waters of the Yellowstone National Park. *US Geol Survey Bull* 47.

Hague, A. 1887. Notes on the deposition of scorodite from arsenical waters in the Yellowstone National Park. *Am J Sci* 34:171-5.

Henley, R.W., A.H. Truesdell, and P.B. Barton, Jr. 1984. Fluid-Mineral Equilibria in Hydrothermal Systems. In vol. 1 of *Reviews of Economic Geology*. El Paso, TX: Economic Geology Publ Co.

Herman, J.S., and M.M. Lorah. 1987. $CO_2$ outgassing and calcite precipitation in Falling Spring Creek, Virginia, U.S.A. *Chem Geol* 62:251-62.

Herman, J.S., and M.M. Lorah. 1988. Calcite precipitation rates in the field: Measurement and prediction for a travertine-depositing stream. *Geochim Cosmochim Acta* 52:2347-55.

Inskeep, W.P., R.E. Macur, G. Harrison, B.C. Bostick, and S. Fendorf. 2004. Biomineralization of As(V)-hydrous ferric oxyhydroxide mats in an acid-sulfate-chloride geothermal spring of Norris Geyser Basin, Yellowstone National Park. *Geochim Cosmochim Acta* 68:3141-55.

Jackson, C.R., H. Langner, J. Christiansen, W.P. Inskeep, and T.R. McDermott. 2001. Molecular analysis of the microbial community involved in arsenite oxidation in an acidic, thermal spring in Yellowstone National Park. *Appl Environ Microbiol* 3:532-42.

Jones, M.E. 1963. Ammonia equilibrium between vapor and liquid aqueous phases at elevated temperatures. *J Phys Chem* 67:1113-15.

Langmuir, D. 1997. *Aqueous Environmental Geochemistry*. Upper Saddle River, NJ: Prentice-Hall.

Langner, H.W., C.R. Jackson, T.R. McDermott, and W.P. Inskeep. 2001. Rapid oxidation of arsenite in a hot spring ecosystem, Yellowstone National Park. *Environ Sci Technol* 35:3302-9.

Macur, R.E., H.W. Langner, B.D. Kocar, and W.P. Inskeep. 2004. Linking geochemical processes with microbial community analysis: Successional dynamics in an arsenic-rich, acid-sulfate-chloride geothermal spring. *Geobiology* 2:163-77.

McCleskey, R.B., D.K. Nordstrom, and J.W. Ball. 2003. Metal interferences and their removal prior to the determination of As(T) and As(III) in acid mine waters by hydride generation atomic absorption spectrometry. *US Geol Surv Water-Resources Investigations Rep* 03-4117.

McCleskey, R.B., D.K. Nordstrom, and A.S. Maest. 2004. Preservation of water samples for arsenic (III/V) determinations: an evaluation of the literature and new analytical results. *Appl Geochem* 19:995-1009.

McCleskey, R.B., J.W. Ball, D.K. Nordstrom, J.M. Holloway, and H.E. Taylor. 2005. Water-Chemistry Data for Selected Springs, Geysers, and Streams in Yellowstone National Park, Wyoming, 2001-2002. *US Geol Surv Open-File Rep* 2004-1316.

Morin, G., F. Juillot, C. Casiot, O. Bruneel, J. Personné, F. Elbaz-Poulichet, M. Leblanc, P. Ildefonse, and G. Calas. 2003. Bacterial formation of tooeleite and mixed arsenic(III) or arsenic(V)-iron(III) gels in the Carnoulès acid mine drainage, France. A XANES, XRD, and SEM study. *Environ Sci Technol* 37:1705-12.

Moses, C.O., D.K. Nordstrom, and A.L. Mills. 1984. Sampling and analysing mixtures of sulphate sulphite, thiosulphate and polythionate. *Talanta* 31:331-9.

Nordstrom, D.K. 2003. Effects of microbiological and geochemical interactions in mine drainage. In *Environmental Aspects of Mine Wastes*, vol. 31, ed. J.L. Jambor, D.W. Blowes, and A.I.M. Ritchie, 227-238. Vancouver, BC: Mineralogical Association of Canada Short Course Series.

Nordstrom, D.K., and J.L. Munoz. 1994. *Geochemical Thermodynamics*. Cambridge, MA: Blackwell Science.

Nordstrom, D.K., J.W. Ball, and R.B. McCleskey. 2003. Orpiment solubility equilibrium and arsenic speciation for a hot spring at Yellowstone National Park using revised thermodynamic data. Abstract from the Geological Society of America Annual Meeting, Seattle, WA.

O'Brien, D.J., and F.B. Birkner. 1977. Kinetics of oxygenation of reduced sulfur species in aqueous solution. *Environ Sci Technol* 11:1114-20.

Raymahashay, B.C. 1968. A geochemical study of rock alteration by hot springs in the Paint Pot Hill area, Yellowstone Park. *Geochim Cosmochim Acta* 32:499-522.

Rochette, E.A., B.C. Bostick, G. Li, and S. Fendorf. 2000. Kinetics of arsenate reduction by dissolved sulfide. *Environ Sci Technol* 34:4714-20.

Rodman, A., H. Shovic, and D. Thoma. 1996. *Soils of Yellowstone National Park,* YCR-NRSR-96-2. Yellowstone National Park, WY: Yellowstone Center for Resources.

Rosholt, J.N. 1976. $^{230}Th/^{234}U$ dating of travertine and caliche rinds. *Geol Soc Am Abs with Programs* 8:1076.

Sorey, M.L. 1991. Effects of potential geothermal development in the Corwin Springs known geothermal resources area, Montana, on the thermal features of Yellowstone National Park. *US Geol Surv Water-Resources Investigations Rep* 91-4052.

Stookey, L.L. 1970. Ferrozine - a new spectrophotometric reagent for iron. *Anal Chem* 42:779-81.

Sturchio, N.C. 1990. Radium isotopes, alkaline earth diagenesis, and age determination of travertine from Mammoth Hot Springs, Wyoming, U.S.A. *Appl Geochem* 5:631-40.

Sturchio, N.C., K.L. Pierce, M.T. Murrell, and M.L. Sorey. 1994. Uranium-series ages of travertines and timing of the last glaciation in the northern Yellowstone area, Wyoming-Montana. *Quatern Res* 41:265-77.

To, T.B., D.K. Nordstrom, K.M. Cunningham, J.W. Ball, and R.B. McCleskey. 1999. New method for the direct determination of dissolved Fe(III) concentration in acid mine waters. *Environ Sci Technol* 33:807-13.

Weed, W.H., and L.V. Pirsson. 1891. Occurrence of sulphur, orpiment, and realgar in the Yellowstone National Park. *Am J Sci* 42:401-5

White, D.E., L.J.P. Muffler, and A.H. Truesdell. 1971. Vapor-dominated hydrothermal systems compared with hot-water systems. *Econ Geol* 66:75-97.

White, D.E., R.A. Hutchinson, and T.E.C. Keith. 1988. The geology and remarkable thermal activity of Norris Geyser Basin, Yellowstone National Park. *US Geol Surv Prof Pap* 1456.

Wilkie, J.A., and J.G. Hering. 1998. Rapid oxidation of geothermal arsenic (III) in streamwaters of the eastern Sierra Nevada. *Environ Sci Technol* 32:657-62.

Xu, Y., and M.A.A. Schoonen. 1995. The stability of thiosulfate in the presence of pyrite in low-temperature aqueous solutions. *Geochim Cosmochim Acta* 59:4605-22.

Xu, Y., M.A.A. Schoonen, D.K. Nordstrom, K.M. Cunningham, and J.W. Ball. 1998. Sulfur geochemistry of hydrothermal waters in Yellowstone National Park: I. The origin of thiosulfate in hot spring waters. *Geochim Cosmochim Acta* 62:3729-43.

Xu, Y., M.A.A. Schoonen, D.K. Nordstrom, K.M. Cunningham and J.W. Ball. 2000. Sulfur geochemistry of hydrothermal waters in Yellowstone National Park: II. Formation and decomposition of thiosulfate and polythionate in Cinder Pool. *J Volcanol Geotherm Res* 97:407-23.

Zhang, J.-Z., and F.J. Millero. 1994. Kinetics of oxidation of hydrogen sulfide in natural waters. In *Environmental Geochemistry of Sulfide Oxidation*, ed. C.N. Alpers and D.W. Blowes, 393-409. Washington, DC: American Chemical Society Symposium Series 550.